GAP 2023 – 018

Updated limits to the UHE neutrino flux from Gamma-Ray Bursts with the Pierre Auger Observatory

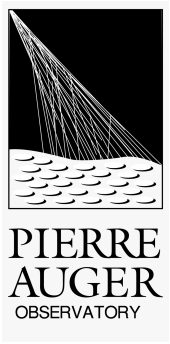

Jaime Alvarez-Muñiz, Yago Lema-Capeáns

Instituto Galego de Física de altas Enerxías (IGFAE)
Universidade de Santiago de Compostela, Spain,

May 16, 2023

Abstract

Since no neutrino candidates have been identified so far in Auger data, we report on an update to the individual and stacking fluence limits from neutrinos from Gamma-ray Bursts (GRBs) with the Surface Detector of the Pierre Auger observatory. The limits are obtained assuming the Waxman-Bahcall model of prompt neutrino emission in the GRB fireball that, at EeV energies, predicts a neutrino energy spectrum $dN_\nu/dE_\nu \propto E_\nu^{-4}$. We have identified a sample of 685 GRBs between 1 Jan 2004 and 31 Dec 2021 in the field-of-view of the Surface Detector array, accounting for both the Earth-Skimming and the Downward-going high-angle channels that are the most sensitive to neutrinos. As a result of extending the data period and hence the number of GRBs in the sample, and of including the Earth-Skimming channel, we have improved by several orders of magnitude the stacking limit with respect to that reported in [1], reducing the difference between the limit and the theoretical prediction of Waxman-Bahcall to a factor $\simeq 5$.

1. Introduction

The sources of Ultra-High Energy (UHE) cosmic rays, although believed to be extragalactic [2], remain unknown. Among them, Gamma-Ray Bursts (GRBs) have been promising candidates due to their extremely large energy release over very short time scales [3]. Proposals to explain the gamma ray emission from GRB, also predict UHE neutrinos, as a consequence of collisions of accelerated protons and nuclei with matter and photons in the GRB [4]. Their detection would be a major step in the discovery of UHE cosmic rays sources.

Neutrinos are neutral and weakly-interacting particles capable of traveling very long distances and escaping dense astrophysical environments, while retaining directional information on the sources where they were produced. This provides a means to identify and study the extreme environments producing cosmic rays. These properties make them almost perfect messengers for Multimessenger Astronomy.

The Surface Detector (SD) of the Pierre Auger Observatory was built to detect UHE cosmic rays, but UHE neutrinos might be identified too [5]. The identification procedure takes advantage of the fact that since neutrinos have a very large mean free path, they can interact at any depth in the atmosphere or when traversing the Earth near the horizon. If a shower is produced near the ground, and it is sufficiently inclined (zenith angle $\theta > 60^\circ$), the electromagnetic component would be significant at ground, while a cosmic-ray induced inclined cascade is very unlikely to produce the same effect. Observables that measure the time duration of traces in the tanks, indicative of signals spreading in time characteristic of the presence of electromagnetic component, are defined and used to identify neutrino showers in [5].

No neutrino candidates have been identified in data collected with the SD of Auger so far [5]. Besides placing limits to the diffuse UHE neutrino flux, it is possible to place limits to point-like sources [6]. In this note, we update the fluence limits for GRBs with respect to the result obtained in 2012 in [1]. We have used data from the SD of the Pierre Auger observatory up to 31 December 2021 where no neutrinos have been identified and included both the Downward-going high (DGH) channel corresponding to $75^\circ < \theta < 90^\circ$ and the Earth-Skimming (ES) channel corresponding to $90^\circ < \theta < 95^\circ$.

This GAP note is structured as follows. In Section 2 we briefly explain the theoretical flux model considered for prompt neutrino emission from GRBs. The GRB sample used is described in Section 3. The calculation of the upper limits to individual GRBs is given in Section 4.1. The calculation of stacking limits, as well as a comparison with the previous limits in [1] is shown in Section 4.2.

2. Waxman-Bahcall fireball model of prompt gamma-ray emission in GRBs

One of the most popular models for the origin of UHECR and UHE neutrino production in GRBs is the so-called *fireball* model. Given the fact that the timescales for the variability seen in GRBs require that a significant amount of energy be deposited in a small volume, the enormous thermal pressure that arises when a massive star collapses, creates an expansion of a fireball that passes through the material surrounding the remnant envelope of the star before escaping in the form of a relativistic jet with a Lorentz factor of ~ 100. What is likely to eventually happen is that the initially released material, that may have to escape through some more heavily baryon-loaded material, will move at speeds lower than that released later. The difference in velocities of shells of material ejected at different times creates shocked regions where Fermi-accelerated electrons emit photons through synchrotron radiation [7], originating the bulk of the gamma-ray emission in the GRB. This so-called *prompt* photon emission is typically non-thermal and it is adequately fitted with simple power-law functions. Usually, the best fit model consists of two smoothly joined power-law prescriptions, the so-called Band function [7],

$$\frac{dN_\gamma}{dE_\gamma} \propto \begin{cases} E_\gamma^{-\alpha} & \text{if } E_\gamma < E_{\rm cut} \\ E_\gamma^{-\beta} & \text{if } E_\gamma > E_{\rm cut} \end{cases} \tag{1}$$

Typical values for the spectral indexes are $\alpha \sim 1$ and $\beta \sim 2$. Besides electrons, protons are also expected to be accelerated in the shocks. Interactions of these accelerated protons with the GRB photons create neutrinos. Photoproduction occurs mainly through the Δ^+ resonance [4, 8],

$$p + \gamma \longrightarrow \Delta^+ \longrightarrow \begin{cases} p + \pi^0 \\ n + \pi^+ \end{cases}, \tag{2}$$

and then pions decay, producing photons and neutrinos, via the following chains,

$$\begin{aligned} \pi^0 &\longrightarrow \gamma + \gamma \\ \pi^+ &\longrightarrow \nu_\mu + \mu^+ \\ &\hookrightarrow \mu^+ \rightarrow \bar{\nu}_\mu + \nu_e + e^+. \end{aligned} \tag{3}$$

The fact that the photon energy spectrum has a change of slope at $E_{\rm cut}$ causes the neutrino spectrum to change slope as well. It can be shown that, for typical values, the break in energy for neutrinos caused by the break in photons is at $E_\nu^{b1} \sim 100$ TeV [8]. However, the neutrino spectrum changes slope a second time due to a different reason. Charged pions produced in the intermediate processes in Eq. (2) might radiate too when their synchrotron loss time is comparable to their lifetime in the comoving reference frame of the fireball. This process breaks again the spectrum, which steepens for the highest energies by a factor E_ν^{-2} [8]. The standard energy values for the second break is $E_\nu^{b2} \sim 10$ PeV. Assuming a typical flux for Fermi-accelerated protons $\frac{dN_p}{dE_p} \sim E_p^{-2}$, the neutrino spectrum can be shown to be [8]:

$$\frac{dN_\nu}{dE_\nu} \propto \begin{cases} E_\nu^{\beta-3} \text{ if } E_\nu < E_\nu^{b1} \\ E_\nu^{\alpha-3} \text{ if } E_\nu^{b1} > E_\nu > E_\nu^{b2} \\ E_\nu^{\alpha-5} \text{ if } E_\nu > E_\nu^{b2}. \end{cases} \tag{4}$$

Since the threshold for neutrino detection with the SD of the Pierre Auger Observatory is typically above 100 PeV, all GRBs that we have considered are assumed to produce a neutrino flux given by

$$\frac{dN_\nu}{dE_\nu} = \phi_\nu(E_\nu) = \phi_0 \cdot \left(\frac{E_\nu}{E_0}\right)^{-4} \quad \text{with} \quad E_0 = 1\,\text{GeV}. \tag{5}$$

where we have assumed that $\alpha \sim 1$ in the Band function in Eq. (1).

3. The GRB sample

In this work we took a sample of GRBs from the GRBweb tool [9], which was developed by the IceCube Collaboration to provide a reliable GRB catalog combining information from multiple detectors, like the Fermi Gamma-Ray Space Telescope and the Neils Gehrels Swift Observatory satellites, and ground-based observatories, providing the starting time of the GRB (t_0), its duration (T90) and its position in the sky. In addition, GRBweb uses a set of automated `Python` scripts to update its database on a weekly basis.

In the time period considered in this work from 1 Jan 2004 until 31 Dec 2021, there are 4194 GRBs with known position in the sky, t_0 and time duration T90 in the GRBweb database. We have only selected GRBs with this information as it is necessary for the calculation of the exposure of the SD during the occurrence of the GRB. The sky positions of all the selected GRBs at the trigger time t_0 of each GRB are plotted in Fig. 1 in the Auger horizontal local coordinates altitude (alt) and azimuth (az). In the plot we show the three regions in which UHE neutrinos are searched for according to the three detection channels, Downward-Going-Low angle (DGL in green), Downward-Going-High angle (DGH in blue) and Earth-Skimming (ES in red). T90 histograms of the samples of GRBs in each channel are also shown in Fig. 1. The typical

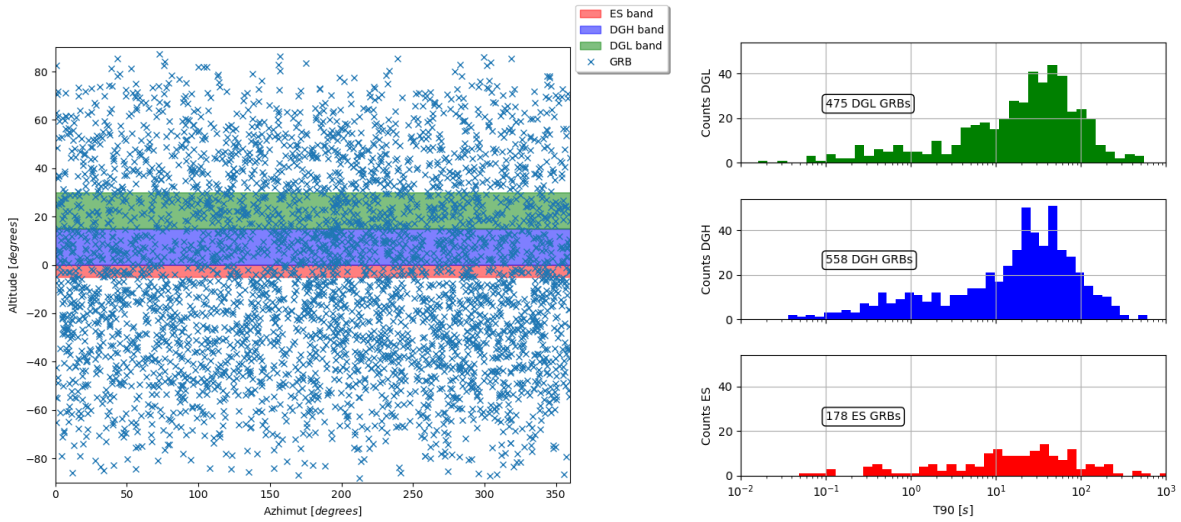

Figure 1: In the left panel we show the sky positions of the 4194 GRBs considered in this work, in the period from 1 Jan 2004 until 31 Dec 2021, plotted in the Auger local horizontal frame (altitude, azimuth) at the trigger time t_0 of each GRB. In the right panel, we show the distribution of the time duration (T90) of the GRBs that have been found to be positioned in one of the three neutrino channel regions (DGL in green, DGH in blue and ES in text - see text). The number of GRBs in each channel is also indicated inside a box in each panel. Note the typical bimodal behaviour of the T90 histogram more apparent in the DGH and DGL channels.

bimodal distribution of T90 corresponding to short and long GRBs is visible, especially in the DGH and DGL channels where the number of GRBs is larger.

We select only the GRBs that are coincident with the field-of-view (FoV) of the Pierre Auger observatory in one of the three neutrino search channels at the trigger time t_0 of each GRB. We reject GRBs occurring during dead-time periods of the SD array. As a consequence, the number of GRBs in the sample gets reduced to 445 in the DGL channel, 517 in the DGH channel and 168 in the ES. The fraction of observation time lost due to the dead-time periods of the SD array is about 13,8%, and all rejected GRBs have their corresponding T90 durations completely contained in a dead-time period. Since the DGL channel is not yet included in this work, a total of 685 GRBs are used, which is more than 10 times the number of GRBs considered in [1]. It is also worth mentioning that there are a few GRBs that, as the Earth rotates during T90, transit across the field-of-view of two search channels. In our entire sample, this is the case for 11 GRBs, and for this reason they are considered twice in the calculation of the exposure, with their corresponding duration times in each channel.

4. Limits to the UHE neutrino fluence from GRBs

4.1. Limits to individual GRBs

In the DGH channel, we compute the effective area of the SD to UHE neutrinos [6] integrating over the array area transverse to the neutrino direction, A, and the atmospheric matter depth of the neutrino trajectory, X, the neutrino identification efficiency, $\varepsilon_{i,c}$, for a neutrino of flavour $i = e, \mu, \tau$ and first interaction of the type c = Charged current (CC), Neutral current (NC), multiplied by the interaction probability per unit depth, $\sigma_c m_p^{-1}$ where m_p is the proton mass and σ_c is the neutrino-nucleon cross section,

$$\mathcal{A}_{i,c}^{\mathrm{DGH}}\left(E_\nu, \theta(t), t\right) = \int_X \int_A \mathrm{d}X \; \mathrm{d}A \; \cos\theta(t) \, \varepsilon_{i,c}\left(\mathbf{r}, E_\nu, \theta(t), D, t\right) \; \sigma_c \, m_p^{-1}. \tag{6}$$

Here, D is the slanted neutrino injection depth (in g cm^{-2}) measured from ground, $\theta(t)$ is the zenith angle of the GRB as seen from the SD array, which in general depends on time t as the Earth rotates and the GRB position in the sky changes. The dependence with time also comes from the number of active tanks of the SD which varies over time.

For the ES channel, the calculation is more complex [6]. We denote as $p_{\rm exit}(E_\nu, E_\tau, \theta)$ the differential probability that a tau neutrino of energy E_ν undergoes a CC interaction along the Earth's chord, and the resulting tau lepton exits to the atmosphere with energy E_τ. This probability along with the identification efficiency ε_{ES} and the tau decay probability per unit length, must be integrated over tau energy E_τ, length l along the τ direction, and surface A to obtain the effective area,

$$\mathcal{A}^{\rm ES}\left(E_\nu, \theta(t), t\right) = \int_{E_\tau}\int_{A}\int_{l} {\rm d}A\ {\rm d}E_\tau \frac{{\rm d}l}{\gamma_\tau \lambda_\tau} \exp\left[-\frac{l}{\gamma_\tau\lambda_\tau}\right] |\cos\theta(t)|\, p_{\rm exit}\, \varepsilon_{\rm ES}, \tag{7}$$

Here $\lambda_\tau \simeq 86.93 \times 10^{-6}$ m is the decay length and γ_τ the Lorentz factor of the tau lepton, assumed to be ultra-relativistic.

Assuming GRBs emit a steady UHE neutrino flux in a time interval T90, the exposure $\mathcal{E}$ is obtained integrating the effective area over T90,

$$\mathcal{E}(E_\nu) = \int_{{\rm T90}_{\rm GRB}} {\rm d}t\, \mathcal{A}\left(E_\nu, \theta(t), t\right). \tag{8}$$

GRBs typically last T90 < 500 s as can be seen in Fig. 1. For the longest ones the corresponding change in zenith angle as viewed from the array is about $\Delta\theta \sim 1.7^o$ for declinations close to the celestial equator. This variation is expected to be less important for GRBs in the DGH channel since the effective area varies relatively slowly with θ in a range of 15°. However, the effect is larger for ES since the effective area changes by roughly 3 orders of magnitude in a narrow region of $\sim 5^\circ$ in zenith angle. We have improved the calculation in [1] by taking into account the time dependence of the zenith angle in the effective area in Eqs. (6) and (7).

Adopting a maximal $\nu_\tau \leftrightarrow \nu_\mu$ mixing, leading to the same fraction of the three neutrino flavours at Earth, the combined exposure for a single GRB in the DGH channel to which all flavours contribute is,

$$\begin{aligned}\mathcal{E}^{\rm DGH}_{\rm GRB}(E_\nu) &= \sum_{i,c} \mathcal{E}^{\rm DGH}_{i,c,{\rm GRB}}\left(E_\nu\right) = \\ &= \sum_{i,c} \int_{T90_{\rm GRB}}\int_X\int_A {\rm d}t\ {\rm d}X\ {\rm d}A\ \cos\theta(t)\, \varepsilon_{i,c}\left(\mathbf{r}, E_\nu, \theta(t), D, t\right)\ \sigma_c\, m_p^{-1}.\end{aligned} \tag{9}$$

The total exposure for a single GRB is obtained adding the exposures of the DGH channel in Eq. (9) and the ES channel obtained after inserting the effective area in Eq. (7) into Eq. (8),

$$\mathcal{E}_{\rm GRB}(E_\nu) = \mathcal{E}^{\rm ES}_{\rm GRB}\left(E_\nu\right) + \sum_{i,c} \mathcal{E}^{\rm DGH}_{i,c,{\rm GRB}}\left(E_\nu\right). \tag{10}$$

The calculation of the effective area of the surface detector is very computationally intensive because the SD array has been growing until deployment finished in 2008, and because of changes in the number of stations working at each instant. In order to simplify the calculation, the effective area of the SD to UHE neutrinos in both the DGH and ES channels is calculated for a set of reference array configurations $\mathcal{A}_{\rm ref}$, assumed to be constant during periods of 3 days, and which correspond to a conservative estimate of the effective area during that period [10]. For each GRB, we use the reference configuration in the 3-day period in which the GRB occurred for the calculation of the effective area, and correct it with the ratio of the actual number of active stations at the time of the GRB[1], $N^{\text{T2-file}}_{\rm stations}$, to the number of active stations in the reference 3-day period, $N^{\rm ref}_{\rm stations}$,

[1] This number can be obtained from the T2-activity files.

$$\mathcal{A}(\theta(t),t) = \frac{N_{\text{stations}}^{\text{T2-file}}(t)}{N_{\text{stations}}^{\text{ref}}}\,\mathcal{A}_{\text{ref}}(\theta(t)). \tag{11}$$

In this way, $N_{\text{stations}}^{\text{T2-file}}(t)$ approximately accounts for the time dependence of the effective area during the T90 due to the status of the SD. Assuming constant values for $N_{\text{stations}}^{\text{ref}}$ during T90, then the exposure is obtained as

$$\mathcal{E}_{GRB} = \int_{T90} \mathrm{d}t\,\mathcal{A}\left(\theta(t),t\right) = \int_{T90} \mathrm{d}t\;\frac{N_{\text{stations}}^{\text{T2-file}}(t)}{N_{\text{stations}}^{\text{ref}}}\,\mathcal{A}_{\text{ref}}(\theta(t)) \tag{12}$$

We use the exposure given in Eq. (12), and the flux in Eq. (5) to obtain the number of expected events within the Auger energy range,

$$\mathcal{N}_{\text{GRB}}^{\nu} = \int_{E_{\text{min}}}^{E_{\text{max}}} \phi_{0,\text{GRB}}\,\left(\frac{E_\nu}{E_0}\right)^{-4}\,\mathcal{E}_{\text{GRB}}(E_\nu)\,\mathrm{d}E_\nu. \tag{13}$$

Finally, we obtain an energy-integrated limit at 90% CL on the value of k_{GRB} in a Feldman-Cousins approach [11], assuming 0 events and 0 background as,

$$\phi_{0,\text{GRB}} = \frac{2.44}{\int_{E_{\text{min}}}^{E_{\text{max}}}\,\left(\frac{E_\nu}{E_0}\right)^{-4}\,\mathcal{E}_{\text{GRB}}(E_\nu)\,\mathrm{d}E_\nu}. \tag{14}$$

It is also conventional to place limits on the energy fluence $\mathcal{F}_{\text{GRB}}$ proportional to the energy emitted in neutrinos per unit area. These can be obtained from the flux multiplying by E_ν^2 and the duration of the GRB,

$$\mathcal{F}_{\text{GRB}} = E_\nu^2\;\text{T90}_{\text{GRB}}\;\phi_{0,\text{GRB}}\,\left(\frac{E_\nu}{E_0}\right)^{-4} = E_0^2\;\text{T90}_{\text{GRB}}\;\phi_{0,\text{GRB}}\,\left(\frac{E_\nu}{E_0}\right)^{-2}. \tag{15}$$

Another way to proceed instead of adding the exposures following (10) is to obtain individual limits using (14) with exposures for each channel of interaction and neutrino flavour. With this procedure, the limit that takes into account all channels is obtained by means of the following expression,

$$\phi_{0,\text{GRB}} = \frac{1}{\sum_{i,c}\frac{1}{\phi_{0,\,\text{GRB}}^{i,c,\,\text{DGH}}} + \frac{1}{\phi_{0,\text{GRB}}^{\text{ES}}}}. \tag{16}$$

Results for individual energy fluence limits for all selected GRBs in the FoV of the DGH and ES channels are plotted in Fig. 2. It can be seen that the primary factor influencing the individual limits is the zenith angle, as it directly determines the effective area. In fact, the limit to the neutrino flux normalization as a function of zenith angle shown in the third panel of Fig. 2 is very similar to the effective area vs zenith angle in [6], but inverted. The fluctuations seen in the values of ϕ_0 arise from the actual number of active stations and the changes in the GRB zenith angle during T90. Note that the dependence of the limits on the fluence with the duration of the GRB is less important because the T90 factor in Eq. (15) approximately cancels out with the same factor in the exposure in Eq. (8).

4.2. Stacking limits

Besides calculating individual fluence limits to all GRBs, we have placed *aggregate* or *stacking* limits to the neutrino fluence by considering all the selected GRBs. Accounting for all the GRBs in the sample we expect the following total number of events,

$$\mathcal{N}_{\text{GRB}}^{\nu,\text{tot}} = \sum_{\text{GRB}}\mathcal{N}_{\text{GRB}}^{\nu} = \sum_{\text{GRB}}\int_{E_{\text{min}}}^{E_{\text{max}}}\phi_{0,\text{GRB}}\cdot\left(\frac{E_\nu}{E_0}\right)^{-4}\,\mathcal{E}_{\text{GRB}}\left(E_\nu\right)\,\mathrm{d}E_\nu. \tag{17}$$

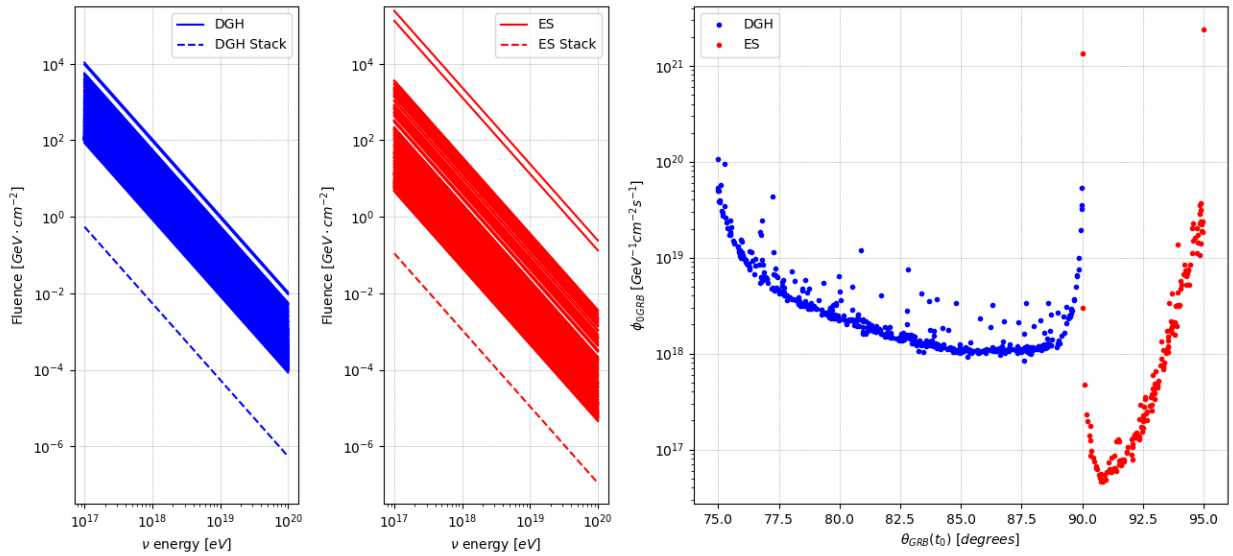

Figure 2: Individual (solid lines) and stacked (dashed lines) GRB fluence limits. Left panel: DGH fluence limits. Middle panel: ES fluence limits. Notice that the limits are up to two orders of magnitude more restrictive in the ES channel than in the DGH one. Right panel: limit to the flux normalization $\phi_{0,\mathrm{GRB}}$ in Eq. (5) as a function of the zenith angle of the GRB at the time of detection of each GRB as obtained in Eq. (14).

For the calculation of the stacking limit to the fluence we firstly denote $\varphi_0^{\mathrm{stack}} = \phi_{0,\mathrm{GRB}}\,\mathrm{T90}_{\mathrm{GRB}}$. With this definition $\mathcal{N}_{\mathrm{GRB}}^{\mathrm{tot}}$ is written as,

$$\mathcal{N}_{\mathrm{GRB}}^{\nu,\mathrm{tot}} = \varphi_0^{\mathrm{stack}} \sum_{\mathrm{GRB}} \int_{E_{\mathrm{min}}}^{E_{\mathrm{max}}} \left(\frac{E_\nu}{E_0}\right)^{-4} \mathcal{E}_{\mathrm{GRB}}\left(E_\nu\right) \frac{1}{\mathrm{T90}_{\mathrm{GRB}}}\,\mathrm{d}E_\nu. \tag{18}$$

Using the Feldman-Cousins approach for 0 events with 0 background, we can place limits to $\varphi_0^{\mathrm{stack}}$ at 90% CL,

$$\varphi_0^{\mathrm{stack}} = \frac{2.44}{\displaystyle\sum_{\mathrm{GRB}} \int_{E_{\mathrm{min}}}^{E_{\mathrm{max}}} \left(\frac{E_\nu}{E_0}\right)^{-4} \mathcal{E}_{\mathrm{GRB}}\left(E_\nu\right) \frac{1}{\mathrm{T90}_{\mathrm{GRB}}}\,\mathrm{d}E_\nu} \tag{19}$$

The stacking fluence limit in this case is obtained simply doing,

$$\mathcal{F}_{\mathrm{stack}} = E_\nu^2\,\varphi_0^{\mathrm{stack}} \left(\frac{E_\nu}{E_0}\right)^{-4} = E_0^2\,\varphi_0^{\mathrm{stack}} \left(\frac{E_\nu}{E_0}\right)^{-2}. \tag{20}$$

The resulting stacking limits for the DGH and ES channels are shown in Figs. 2 and 3. The total stacking limit combining both channels is shown in Fig. 3, along with the Waxman-Bahcall flux prediction for a single GRB[2] scaled to 685 GRBs as in the sample used in this work. With this result we have improved by two orders of magnitude the previous stacking limit in [1], not only because of the increase in the number of GRBs due to the longer data period considered, but also because of the GRBs in the FoV of the ES channel, where the sensitivity to UHE neutrinos is largest in Auger. The difference between the theoretical Waxman-Bahcall prediction and the fluence limit is roughly a factor 5. As a consequence, the Waxman-Bahcall GRB fireball model of neutrino production is getting increasingly constrained.

[2]The fluence of a single WB GRB is calculated from the all-sky diffuse flux from GRB in [4] multiplying by $4\pi\,\mathrm{sr\,yr}$ and dividing by the expected number of bursts per year (667) and dividing by two to account for neutrino oscillations, see [12].

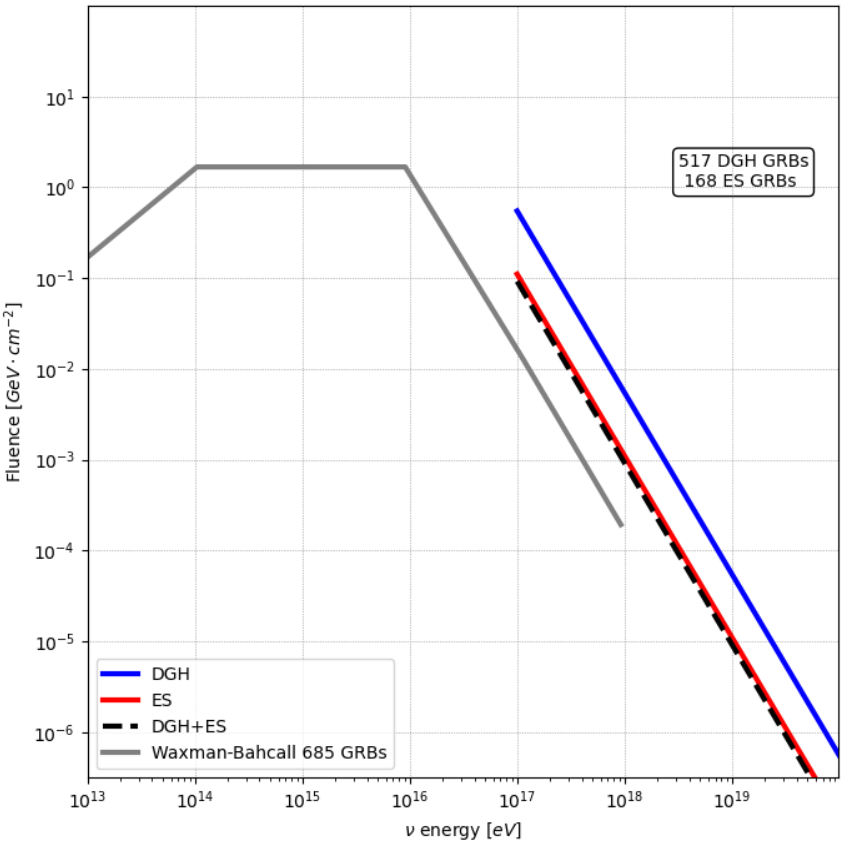

Figure 3: Stacked limits of Prompt neutrinos from GRBs for DGH, ES and combining both channels along with the Waxman-Bahcall prompt model for neutrino production for 685 GRBs (see text).

5. Conclusions

In this note we have placed individual and stacking limits to the prompt UHE neutrino fluence from GRBs with the SD of the Pierre Auger Observatory. We have identified and selected 685 GRBs in the period 1 Jan 04 - 31 Dec 2021 that were in the field of view of Auger sensitive to neutrinos at the time of their detection while the SD array was actively taking data. Out of them, 517 corresponded to the DGH channel and 168 to the ES channel. The limits obtained here have improved the result in [1] by almost three orders of magnitude. The expected fluence of UHE prompt neutrinos in GRBs is still too low to expect a detection, but the constraints on the simple Waxman-Bahcall model are more stringent.

In the future, the DGL channel ($60^\circ < \theta < 75^\circ$) will be included in the calculation, increasing the sample with 445 new GRBs although with the sensitivity in that angular range being smaller than in the DGH and ES channels. We will also consider more realistic numerical calculations of the flux of UHE neutrinos from GRBs based on the fireball model [13] taking into account the full energy dependencies of the proton and photon spectra as well as the cooling of the secondary pions and additional multipion production beyond the $\Delta-$resonance. Afterglow models (see for instance [14]), predicting UHE neutrinos, will also be considered.

References

[1] J. Alvarez-Muñiz et al. "Limits to the UHE neutrino flux from Gamma-Ray Bursts with the Pierre Auger Observatory". In: *GAP-2012-064* (2012).

[2] Alexander Aab et al. "Observation of a Large-scale Anisotropy in the Arrival Directions of Cosmic Rays above 8×10^{18} eV". In: *Science* 357.6537 (2017), pp. 1266–1270. DOI: 10.1126/science.aan4338. arXiv: 1709.07321 [astro-ph.HE].

[3] Mario Vietri. "On the acceleration of ultrahigh-energy cosmic rays in gamma-ray bursts". In: *Astrophys. J.* 453 (1995), pp. 883–889. DOI: 10.1086/176448. arXiv: astro-ph/9506081.

[4] Eli Waxman and John Bahcall. "High Energy Neutrinos from Cosmological Gamma-Ray Burst Fireballs". In: *Phys. Rev. Lett.* 78 (12 Mar. 1997), pp. 2292–2295. DOI: 10.1103/PhysRevLett.78.2292. URL: https://link.aps.org/doi/10.1103/PhysRevLett.78.2292.

[5] Alexander Aab et al. "Probing the origin of ultra-high-energy cosmic rays with neutrinos in the EeV energy range using the Pierre Auger Observatory". In: *JCAP* 10 (2019), p. 022. DOI: 10.1088/1475-7516/2019/10/022. arXiv: 1906.07422 [astro-ph.HE].

[6] A. Aab et al. "Limits on point-like sources of ultra-high-energy neutrinos with the Pierre Auger Observatory". In: *Journal of Cosmology and Astroparticle Physics* 2019.11 (Nov. 2019), p. 004. DOI: 10.1088/1475-7516/2019/11/004. URL: https://dx.doi.org/10.1088/1475-7516/2019/11/004.

[7] Andrew Levan. *Gamma-Ray Bursts*. 2514-3433. IOP Publishing, 2018. ISBN: 978-0-7503-1502-9. DOI: 10.1088/2514-3433/aae164. URL: https://dx.doi.org/10.1088/2514-3433/aae164.

[8] D. Guetta et al. "Neutrinos from individual gamma-ray bursts in the BATSE catalog". In: *Astroparticle Physics* 20.4 (2004), pp. 429–455. ISSN: 0927-6505. DOI: https://doi.org/10.1016/S0927-6505(03)00211-1. URL: https://www.sciencedirect.com/science/article/pii/S0927650503002111.

[9] P. Narayana Bhat et al. "The third Fermi GBM Gamma-Ray Burst Catalog: The first six years". In: *The Astrophysical Journal Supplement Series* 223.2 (Apr. 2016), p. 28. DOI: 10.3847/0067-0049/223/2/28. URL: https://dx.doi.org/10.3847/0067-0049/223/2/28.

[10] J. Alvarez-Muñiz *et al.* "A limit on the diffuse flux of UHE neutrinos with down-going showers from the Pierre Auger Observatory". In: *GAP-2008-054* (2008).

[11] Gary J. Feldman and Robert D. Cousins. "Unified approach to the classical statistical analysis of small signals". In: *Phys. Rev. D* 57 (7 Apr. 1998), pp. 3873–3889. DOI: 10.1103/PhysRevD.57.3873. URL: https://link.aps.org/doi/10.1103/PhysRevD.57.3873.

[12] R. Abbasi et al. "Search for muon neutrinos from Gamma-Ray Bursts with the IceCube neutrino telescope". In: *Astrophys. J.* 710 (2010), pp. 346–359. DOI: 10.1088/0004-637X/710/1/346. arXiv: 0907.2227 [astro-ph.HE].

[13] Svenja Hummer, Philipp Baerwald, and Walter Winter. "Neutrino Emission from Gamma-Ray Burst Fireballs, Revised". In: *Phys. Rev. Lett.* 108 (2012), p. 231101. DOI: 10.1103/PhysRevLett.108.231101. arXiv: 1112.1076 [astro-ph.HE].

[14] Jessymol K. Thomas, Reetanjali Moharana, and Soebur Razzaque. "Ultrahigh energy neutrino afterglows of nearby long duration gamma-ray bursts". In: *Phys. Rev. D* 96.10 (2017), p. 103004. DOI: 10.1103/PhysRevD.96.103004. arXiv: 1710.04024 [astro-ph.HE].